Supporting Information

Mitofusin-Decorated Extracellular Vesicles Enable Targeted Nucleic Acid Delivery to Mitochondria

Jiafeng Zhong[1,2], Luyao Wang[3,*], Wenjing Xuan[3], Xuehan Xu[3], Xing Chang[2], Jianjun Cheng[3,4,5,*], Chengjie Sun[3,*]

[1]Fudan University, Shanghai 200433, China

[2]School of Medicine, Westlake University, Hangzhou, Zhejiang 310023, China

[3]Department of Materials Science and Engineering, Westlake University, Hangzhou, Zhejiang 310030, China

[4]Research Center for Industries of the Future, Westlake University, Hangzhou, Zhejiang 310030, China

[5]Institute of Advanced Technology, Westlake Institute for Advanced Study, Hangzhou, Zhejiang 310024, China

*Correspondence:

wangluyao@westlake.edu.cn;
chengjianjun@westlake.edu.cn;
sunchengjie@westlake.edu.cn

Materials and Methods

Animals

BALB/c-nude mice were obtained from the Laboratory Animal Resources Center of Westlake University. All mice were housed in standard specific pathogen-free (SPF) conditions. The study protocols were reviewed and approved by the Institutional Animal Care and Use Committee (IACUC) at the School of Life Sciences, Westlake University (AP#21-051). All animal experiments were conducted following the guidelines in the “Guide for the Care and Use of Laboratory Animals”.

Cell culture

HEK 293T and HeLa cells were obtained from the High-Throughput Core Facility of Westlake University and cultured in Dulbecco's Modified Eagle Medium (DMEM, Wisent. Inc) supplied with 10% fetal bovine serum (FBS, Wisent. Inc), penicillin (100 units/mL, Wisent. Inc) and streptomycin (100 μg/mL, Wisent. Inc) in an incubator with a 5% CO_2 atmosphere at 37 °C.

Plasmids construction

Original plasmids pLV3-CMV-LAMP2B-HA-Hygro, pCMV-MFN1-FLAG-Neo, pCMV-MFN2(human)-FLAG-WPRE-Neo, pU6-sgRNA-CMV-Cas9-SV40-mCherry-IRES-Puro, pLV2-CMV-Mito-EGFP-Puro, psPAX2, pMD2.G were purchased from Miaoling Bio. To generate plasmid encoding CD63-Nluc fusion protein, the sequence of human CD63 and NanoLuc luciferase were got from NCBI gene bank and the combined fragment was synthesized by Tsingke Biotechnology and cloned into a lentiviral pLVX vector. To create the plasmid expressing MFN1-LAMP2B or MFN2-LAMP2B, the pLV3-CMV-LAMP2B-HA-Hygro backbone was linearized by Nsi I enzyme (R0127, New England Biolabs) digestion and the MFN1 or MFN2 sequence was PCR amplified and cloned into the restriction site using the In-Fusion Snap Assembly Master Mix Kit (638947, Takara). The MFN2-LAMP2B was then subcloned into pLVX-IRES-puro vector. The same in-fusion method was used to obtain the mitoCas9 plasmid. All plasmid constructs were confirmed by sequencing (Tsingke Biotechnology) before use, and the sequence information was provided in Supplemental Table S1 (primers) and Table S3 (fusion proteins).

Stable cell line construction

HEK 293T cells were co-transfected with psPAX2, pMD2.G and the intended

expressing vectors by Lipofectamine 3000 (L3000015, Thermo Fisher) following the manufacturer's protocol. The transfection medium was refreshed with 3% FBS/1× NEAA (MEM Non-Essential Amino Acids Solution, 11140050, Gibco) DMEM after 6 h. The lentivirus containing supernatants were collected at 72 h and cleared by centrifugation at 1000 *g* for 5 min, then supplied with 8 μg/mL of polybrene (C0351, Beyotime) and 20 mM HEPES (15630106, Gibco) and store at -80 °C if not used immediately.

For lentivirus transduction, HEK 293T cells were seeded in 3% FBS DMEM supplied with 8 μg/mL of polybrene and 20 mM HEPES, which was change to normal culture medium 6 h after the addition of lentivirus containing supernatants. Transduced cells were split into duplicate and indicated antibiotic (puromycin or hygromycin B, HY-B1743, HY-B0490, MCE) was added at 48 h.

After 7-day selection, the transduced cells were diluted to less than 10 cell/mL and seeded into 96-well plates (100 μL each well) for single cell clone screening, and the intended protein expression was further confirmed by PCR and immunoblotting.

EV/MFNEV isolation

For EV/MFNEV production, EV-depleted FBS was prepared by ultracentrifugation at 120000 *g*, 4 °C for 16 h (CP100NX, Himac)and filtration through 0.22 μm filters. The HEK 293T or HEK 293T-MFN1-LAMP2B /MFN2-LAMP2B cells were cultured in DMEM with EV-depleted FBS. Then the conditioned medium was collected and centrifuged at 600 *g* for 5 min, 3000 *g* for 15 min and 10000 *g* for 60 min to remove cell debris and large contaminants. The resulted supernatant was supplied with 10% PEG8000 (HY-Y0873J, MCE) solution and incubated at 4 °C overnight, then centrifuged at 3000 *g* for 60 min. The pellets were resuspended in small volume of cold PBS solution and subjected into an Exosupur (ES914, Echo Biotech) size-exclusion chromatography column. The vesicle-containing fraction was collected following the manufacturer's protocol. Generally, 6–8 mg of EV or MFNEV can be obtained from 500 mL of conditioned medium by the size exclusion chromatography method. The EVs and MFNEVs are stable when stored at -80 °C. Repeated freeze-thaw cycles should be avoided.

EV/MFNEV characterization

The size of EV and MFNEV was detected through the Flow NanoAnalyzer (NanoFCM Inc.).

For detection of the positive ratio of MFN1-LAMP2B and MFN2-LAMP2B on EV or

MFNEV, EVs or MFNEVs were incubated with anti-MFN1-FITC (1:100, sc-166644FITC, SantaCruz) and anti-MFN2-PE (1:100, sc-515647PE, SantaCruz) antibodies on shaker at 4 °C overnight. The unconjugated antibodies were removed by ultracentrifugation and the resulted EVs or MFNEVs were analyzed by Flow NanoAnalyzer. The data was processed with Origin 2021 software.

The morphology was characterized by cryo-electron microscopy. In brief, lacey carbon EM grids were glow-discharged (30 s, 25 mA). 5 μL of purified EV or MFNEV solution was applied onto the carbon side, then blotted for 3.0 s, force 5 and plunge-frozen into the precooled liquid ethane. The samples were visualized on Glacios3 Cryo-TEM (Thermo Fisher).

To detect the EV-associated proteins as well as the fusion protein MFN1-LAMP2B and MFN2-LAMP2B, cells and EV/MFNEV were treated with radioimmunoprecipitation (RIPA, P0013B, Beyotime) buffer and subjected to SDS-PAGE electrophoresis according to the standard immunoblotting procedure. Primary antibodies anti-GM130 (1:1000, ab52649, Abcam), anti-Hsp70 ((1:1000, ab181606, Abcam), anti-CD63 (1:1000, A22343, ABclonal), anti-Flotillin1 (1:1000, A3023, ABclonal), anti-GAPDH (1:2000, abs132004, Absin), anti-MFN1 (1:1000, A21293, ABclonal), anti-MFN2 (1:1000, E-AB-32025, ELabscience) were incubated with the blotted membrane, respectively. The results were visualized on the ChemiDoc Imaging Systems (Bio-Rad).

Cargos packaging via electroporation

The relative protein concentration of purified EVs/MFNEVs was quantified by measuring the absorbance at 280 nm. Then the EV/MFNEV were mixed with indicated siRNAs or sgRNAs at a weight ratio of 20:1, or with RNP at 10:1, respectively. The mixture was then diluted to 0.4 mg/mL with 0.33 M sucrose solution and transferred to 4 mm cuvettes (Bio Rad) on ice. Electroporation was performed at 400 voltage, square wave for three times on the BTX Electroporation System Gemini X2. After electroporation, the solution was incubated at 37 °C for 30 min. The free siRNAs or sgRNAs were removed by ultrafiltration through 100 kDa Amicon filter (Millipore) while the free RNPs were removed by ultracentrifugation at 100000 *g* for 60 min. The encapsulation efficiency was analyzed according to the recovered fluorescence (siRNA, ~25%) or the Quant-iT RiboGreen (R11490, Thermo) Kit (for sgRNA, ~20%).

Intracellular localization of EV/MFNEV

For fluorescence imaging, 4 × 10^5 of HEK 293T-mitoEGFP cells were seeded in 35 mm glass-bottomed dishes. Cy5-labeled siRNA was purchased from GenePharma and loaded in to EV or MFNEV by electroporation as described above. MFNEVs incubated

with anti-MFN1 (1:100, ABclonal) or anti-MFN2 (1:100, ELabscience) antibodies at RT for 30 min were purified by ultracentrifugation. 40 μg of EVs or MFNEVs containing ~0.5 μg of siRNA was added to the cell culture. The cells were stained with Lysotracker Red DND 99 (L7528, Invitrogen) and NucBlue (R37605, Invitrogen) before visualized by laser scanning confocal microscope (LSM980, Carl Zeiss). The Pearson correlation coefficient of EV-mitochondria or EV-lysosome was calculated by the ZEN software. High-resolution mitochondrial images were acquired using a multimodality structured illumination microscopy (Multi-SIM) imaging system (NanoInsights-Tech Co., Ltd.) equipped with a 100×/1.40 NA oil-immersion objective and a Photometrics Kinetix camera.

To further analyze the targeting ability of MFNEV, mitochondria from 1.5×10^6 of HEK 293T treated with EV-siRNA or MFNEV-siRNA (1.6 μg of siRNA) were isolated using Mitochondria Isolation Kit (HY-K1060, MCE), sequentially treated with 1 mg/mL digitonin and RNase (for outer membrane removal), and then digested with proteinase K (P1120, SolarBio) at 37 °C for 30 min. The resulted products were subjected to 2% agarose gel for electrophoresis, and 25 ng of free siRNAs were loaded as control. The gel was imaged on the ChemiDoc Imaging Systems (Bio-Rad). Anti-ERP44 (1:1000, A4526, ABclonal), anti-COX IV (1:1000, A28231, ABclonal), anti-TOM20 (1:1000, A19403, ABclonal) were used for immunoblotting. According to the manufacturers, the anti-MFN1 antibody (A21293, ABclonal) recognizes amino acids 642–741 (helix bundle domain, UniProt Q8IWA4), and the anti-MFN2 antibody (E-AB-32025, Elabscience) recognizes amino acids 354–403 (helix bundle domain, UniProt O95140).

Extracellular vesicle secretion assay

The HEK 293T-CD63Nluc cell was constructed for examining the influence of the transduced fusion proteins on the vesicular secretion. The CD63Nluc cells were seeded at 6×10^4 cells per well in 24-well plates and transfected with indicated plasmids (empty vector, LAMP2B, MFN1-LAMP2B, MFN2-LAMP2B) by Lipo 3000. The culture medium was refreshed after 6 h and the volume was strictly controlled (0.5mL/well) to be same for each group. 48 h after transfection, the culture medium was collected and centrifuged at 3000 *g* for 5 min to remove cells or cell debris. 100 μL of the supernatant was incubated with Furimazine (T15359, TargetMol) solution. The luminescence was detected on the microplate reader (Bio Tek).

Cell proliferation assay

2000 of HEK 293T cells were cultured in 96-well plates overnight and incubated with EV or MFNEV at indicated concentrations of total vesicular protein (0, 0.2, 0.5, 1, 2, 5

μg per 10^4 of cells). The Cell Counting Kit-8 (CCK8, K1018, ApexBio) regent was added after 48 h and 72 h. Cell viability was then determined by measuring the 450 nm absorbance using microplate reader (Bio Tek).

Mitochondrial siRNA delivery *in vitro* and *in vivo*

siRNAs targeting the mitochondrial DNA encoded ND1 (siND1, human), COX2 (siCO2, human) and *Cytb* (siCytb, mouse) were purchased from GenePharma. For *in vitro* experiments, 4×10^5 of HEK 293T or HeLa cells were seeded in 6-well plates with indicated amounts of EV/MFNEV packaged siRNAs. Total RNA was extracted using the Fast Pure Cell/Tissue Total RNA Isolation Kit V2 (RC112, Vazyme) at 24 h and reverse-transcribed into complementary DNA (cDNA) by PrimeScript RT reagent Kit (RR047, Takara). Quantitative PCR (qPCR) was performed on the CFX Connect Real-Time PCR System (Bio-Rad) and TB Green Premix Ex Taq (Tli RNaseH Plus, RR420, Takara) was used for the reactions. The data were analyzed by the ΔΔCt method. Protein samples were collected at 60 h after incubation for western blotting. Primary antibodies anti-MTND1 (1:1000, A17967, ABclonal), anti-Hsp60 (1:1000, 1007-1, Hua Bio) were used for detection.

The biodistribution was assessed by intravenously injection of 100 μg of EV/MFNEV loaded with Cy5-siRNAs into BALB/c nude mice. The mice were euthanized at 24 h and tissues including the liver, heart, lung, spleen, and kidney were excised and imaged using the IVIS Spectrum imaging system (PerkinElmer). Mice treated with 360 μg of EV/MFNEV (containing ~4.5 μg of siCytb) per 20 g bodyweight were sacrificed at 24 h and 120 h, and the liver tissue was excised for total RNA extraction and quantitative analyzing of Cytb mRNA expressing. Blood samples were collected to separate serum for determining the systemic toxicity. Serum levels of ALT and AST were determined using a biochemical autoanalyzer (Toshiba). All the primers used for qPCR were listed in Supplementary Table 1.

Mitochondrial sgRNA/RNP delivery for CRISPR editing

sgDloop, sgND1, sgCO3 and sgGFP were designed by online tools (http://chopchop.cbu.uib.no/) and synthesized by GenScript. Cas9 Nuclease without nuclear localization sequence (NLS) was purchased from GenScript (Z03386). 4×10^5 of HEK 293T or HEK 293T-mitoCas9 cells were incubated with 40 μg of EV/MFNEV containing either ~0.5 μg of RNP or ~0.4 μg of sgRNAs. Total DNA was extracted at 16 h by the Fast Pure Cell/Tissue DNA Isolation Mini Kit (DC102, Vazyme). Human Mitochondrial DNA (mtDNA) Monitoring Primer Set containing primer pairs of ND1, ND5, SLCO2B1, SERPINA1 (7246, Takara) was used for the detection of mtDNA by

qPCR. The average of $2^{\Delta\Delta Ct}$ (ND1 versus SLCO2B1) and $2^{\Delta\Delta Ct}$ (ND5 versus SERPINA1) was used as the relative mtDNA content (normalized to the sgGFP group).

Data analysis

The data from Flow NanoAnalyzer was processed with Origin 2021 software. The sequence identity and similarity of human/mouse MFN1 and MFN2 were compared using SnapGene v8.0. GraphPad Prism 8.0 was used for all statistical analysis. All results are expressed as mean ± SD The statistical significance was analyzed by Student's *t* test or analysis of variance (ANOVA). $P < 0.05$ was considered significant. ns, $P > 0.05$; *$P < 0.05$, **$P < 0.01$, ***$P < 0.001$.

Table S1. Sequence information of primers

Primers	Sequence (5'-3')	Notes
MFN1-LAMP2B_F	AGCTGTGCGGTCTTATGCCACCATGGCAGAACCT	In-fusion cloning of MFN1-LAMP2B
MFN1-LAMP2B_R	CAAATTAAGTTCCAAGGATCCGGATTCTTCATTGCT	
MFN2-LAMP2B_F	AGCTGTGCGGTCTTACGCCACCATGTCCCTGCT	In-fusion cloning of MFN2-LAMP2B
MFN2-LAMP2B_R	CAAATTAAGTTCCAACTCGAGTCTGCTGGGCTG	
COX8MTS_F	TCGAGCTCAAGCTTCGAATTATGTCCGTCCTGACGCCG	In-fusion cloning of mitoCas9
COX8MTS_R	ACTTCTTGTCCAACGAATGGATCTTGGCGCG	
CAS9_F	CCATTCGTTGGACAAGAAGTACAGCATCGGCC	
CAS9_R	GTACCGTCGACTGCAGAATTTCAGGAGCCGCCGTCGCCGCC	
MFN1LM_sF	GAGCGAGCCTTTAAACAGCAG	Verification for positive cell line
MFN1LM_sR	CAGGAAAAGCCAGGTCCGAA	
MFN2LM_sF	TGTCTGGGACCTTTGCTCATC	Verification for positive cell line
MFN2LM_sR	GCTGCCTTGGTAAAATTCGCA	
mitoCas9_sF	CCAAGATCCATTCGTTGGACAAG	Verification for positive cell line
mitoCas9_sR	GTAGCCGTTCTTGCTCTGGT	
16S rRNA_F	TACCCCGCCTGTTTACCA	qPCR
16S rRNA_R	GGCAGGTCAATTTCACTGG	qPCR
ND1_F	GAACAACATATGACGCACTC	qPCR
ND1_R	GGTGTATGAGTTGGTCGTAG	qPCR
COX2_F	AGTCCTCATCGCCCTC	qPCR
COX2_R	CTCGTAGGTTCAGTACCATTG	qPCR
ATP6_F	TGCCTCACTCATTTACACCAAC	qPCR
ATP6_R	ATGGTTGATATTGCTAGGGTGG	qPCR
Ms16S rRNA _F	CGAGCTTGGTGATAGCTGGT	qPCR
Ms16S rRNA _R	GAGCTGTCCCTCTTTTGGCT	qPCR
MsCytb_F	GCCCTAGCAATCGTTCACCT	qPCR
MsCytb_R	ATGGGGTGGGGTGTTTAGTG	qPCR

Table S2. Sequence information of siRNAs and sgRNAs

siRNAs	**sense (5'-3')**	**antisense (5'-3')**
siND1-1	GCCGAAUACACAAACAUUATT	UAAUGUUUGUGUAUUCGGCTT
siND1-2	GCCGAAUACACAAACAUUATT	UAAUGUUUGUGUAUUCGGCTT
siND1-3	GCCGAAUACACAAACAUUATT	UAAUGUUUGUGUAUUCGGCTT
siCO2-1	CCCUACGCAUCCUUUACAUTT	AUGUAAAGGAUGCGUAGGGTT
siCO2-2	GGACUAAUCUUCAACUCCUTT	AGGAGUUGAAGAUUAGUCCTT
siCO2-3	CUACGGUCAAUGCUCUGAATT	UUCAGAGCAUUGACCGUAGTT
siCytb-1	GGGUGACUAAUCCGAUAUATT	UAUAUCGGAUUAGUCACCCTT
siCytb-2	GGUAUCCUAAUCAUAUUCUTT	AGAAUAUGAUUAGGAUACCTT
siCytb-3	GCCAACCUACUUAUCUUAATT	UUAAGAUAAGUAGGUUGGCTT
siNT	UUCUCCGAACGUGUCACGUTT	ACGUGACACGUUCGGAGAATT
siOPA1	AAGUUAUCAGUCUGAGCCAGG UUTT	AACCUGGCUCAGACUGAUAAC UUTT
siMFN1-1	GGAGCUCAAAGUUGUAAAUTT	AUUUACAACUUUGAGCUCCTT
siMFN1-2	CGGCUUUCCAAGCCUAAUATT	UAUUAGGCUUGGAAAGCCGTT
siMFN1-3	GGCACUUGCUGAAGGAUUUTT	AAAUCCUUCAGCAAGUGCCTT
siMFN2-1	CUGCGAAUUAAGCAGAUUATT	UAAUCUGCUUAAUUCGCAGTT
siMFN2-2	CCCUCAACUAUGACCUAAATT	UUUAGGUCAUAGUUGAGGGTT
siMFN2-3	CUGCAGUGAAGACCAAGUUTT	AACUUGGUCUUCACUGCAGTT
Cy5-siNT	Cy5-UUCUCCGAACGUGUCACGUTT	Cy5-ACGUGACACGUUCGGAGAATT
sgRNAs	**Sequence (5'-3')**	
sgND1	CGTAGGGGCCTACAACGTTGGUUUUAGAGCUAGAAAUAGCAAGUUAAA AUAAGGCUAGUCCGUUAUCAACUUGAAAAAGUGGCACCGAGUCGGUG CUUUU	
sgCO3	TGTTGAGCCGTAGATGCCGTGUUUUAGAGCUAGAAAUAGCAAGUUAAA AUAAGGCUAGUCCGUUAUCAACUUGAAAAAGUGGCACCGAGUCGGUG CUUUU	
sgDloop	GCACCTACGTTCAATATTACGUUUUAGAGCUAGAAAUAGCAAGUUAAAA UAAGGCUAGUCCGUUAUCAACUUGAAAAAGUGGCACCGAGUCGGUGC UUUU	
sgGFP	AGTAGTCGACGATGTCCTGGGUUUUAGAGCUAGAAAUAGCAAGUUAAA AUAAGGCUAGUCCGUUAUCAACUUGAAAAAGUGGCACCGAGUCGGUG CUUUU	

Table S3. Sequence information of fusion proteins

Sequence (5'-3')
MFN1-LAMP2B: ATGTGCGGCCCCAACCGCCGCGGCGACTGCATGGTGTGCTTCCGCCTCTTCCC GGTTCCGGGCTCAGGGCTCGTTCTGGTCTGCCTAGTCCTGGGAGCTGTGCGGT CTTATGCCACC(LAMP2B)***atggcagaacctgtttctccactgaagcactttgtgctggctaagaaggc gattactgcaat…*****(MFN1)*****…tggagaattttactaagcagtttctaccttcaagcaatgaagaatccggatc c***TTGGAACTTAATTTGACAGATTCAGAAAATGCCACTTGCCTTTATGCAAAATGGC AGATGAATTTCAC…(LAMP2B)
MFN2-LAMP2B: ATGTGCGGCCCCAACCGCCGCGGCGACTGCATGGTGTGCTTCCGCCTCTTCCC GGTTCCGGGCTCAGGGCTCGTTCTGGTCTGCCTAGTCCTGGGAGCTGTGCGGT CTTACGCCACC(LAMP2B)***atgtccctgctcttctctcgatgcaactctatcgtcacagtcaagaaaaat aagagacacat…*****(MFN2)*****…tgagctcaacatgttcacacaccagtacctgcagcccagcagactcgag*** TTGGAACTTAATTTGACAGATTCAGAAAATGCCACTTGCCTTTATGCAAAATGGCA GATGAATTTCACAGTA…(LAMP2B)
CD63Nluc: ATGGCGGTGGAAGGAGGAATGAAATGTGTGAAGTTCTTGCTCTACGTCCTCCTG CTGGCCTTTTGCGCCTGTGCAGT…(CD63)…GTGAAGAGTATCAGAAGTGGCTAC GAGGTGATG*gctagcagtggctctggt***ATGGTCTTCACACTCGAAGATTTCGTTGGGGAC TGGCGACAGACAGCCGGCTACAACCTGGACCAA…(NanoLuc)**
mitoCas9: ATGTCCGTCCTGACGCCGCTGCTGCTGCGGGGCTTGACAGGCTCGGCCCGGC GGCTCCCAGTGCCGCGCGCCAAG(MTS)*atccattcgttg***GACAAGAAGTACAGCATC GGCCTGGACATCGGTACCAACAGCGTGGGCTGGGCCGTGATCACCGACGAGT ACAAGGTGCCCAGCAAGAAGTTCAAGGTGCTGGGCAACACCG…(spCs9)**

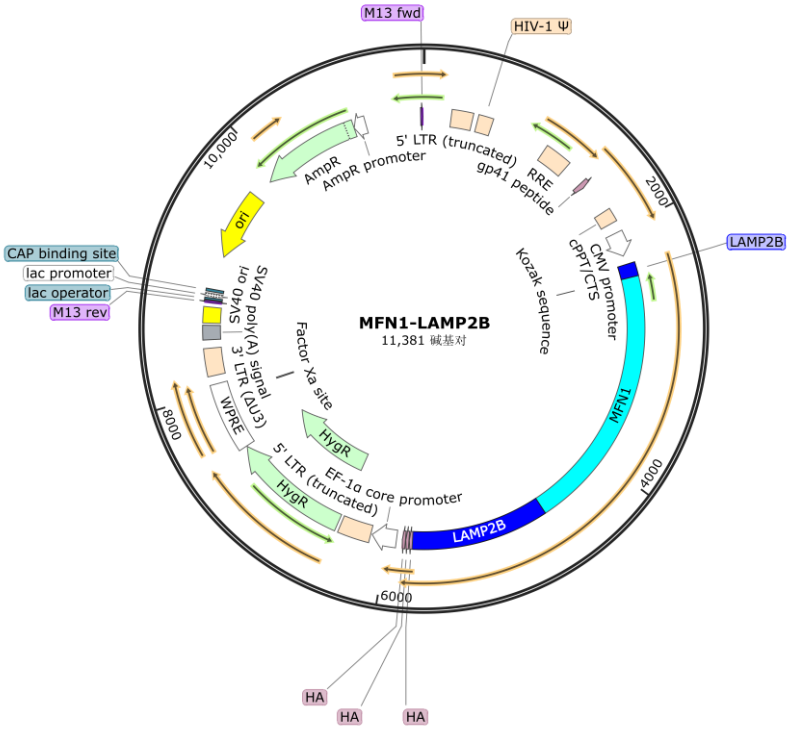

Figure S1. Plasmid map of MFN1-LAMP2B DNA vector.

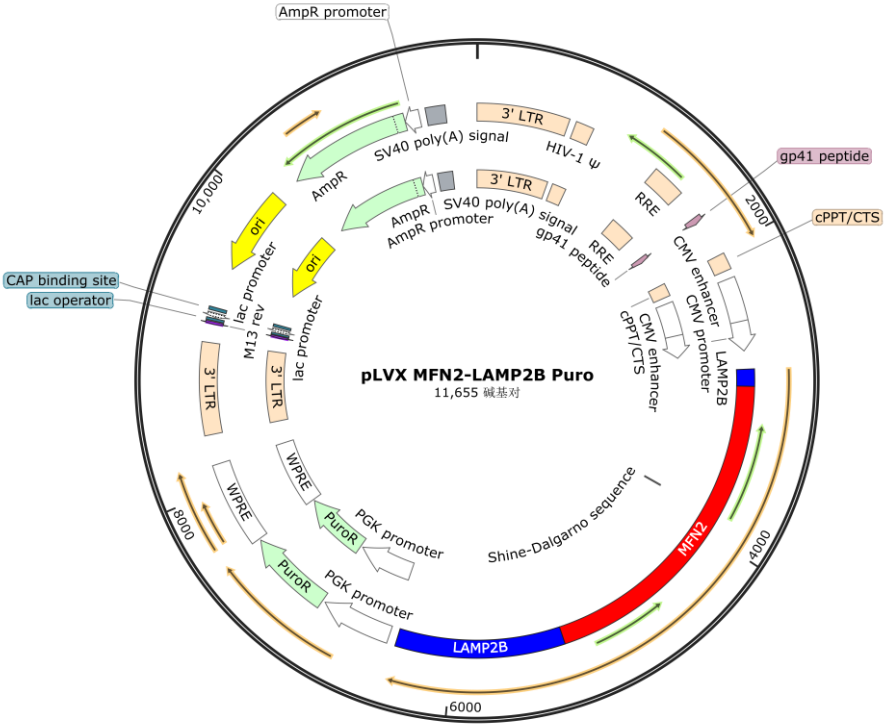

Figure S2. Plasmid map of MFN2-LAMP2B DNA vector.

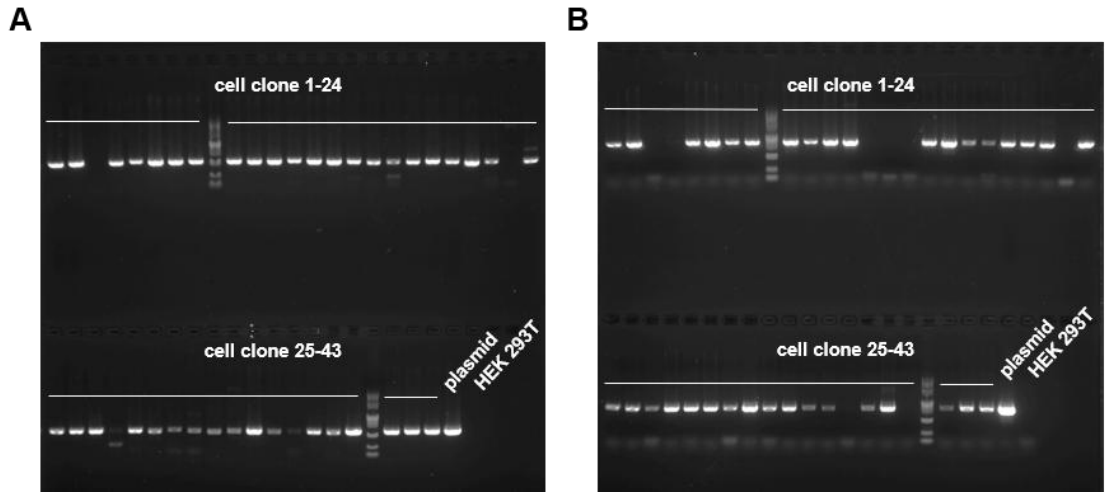

Figure S3. Screening of single cell clones of HEK 293T MFN1-LAMP2B /MFN2-LAMP2B double positive cells. Single cell clones in 96-well plates were analyzed by PCR reaction of the (**A**) MFN1-LAMP2B and (**B**) MFN2-LAMP2B fragments. The last two channels used the plasmids and un-transduced HEK 293T cell as template for positive and negative control. The primer sequence was provided in Supplementary Table S1.

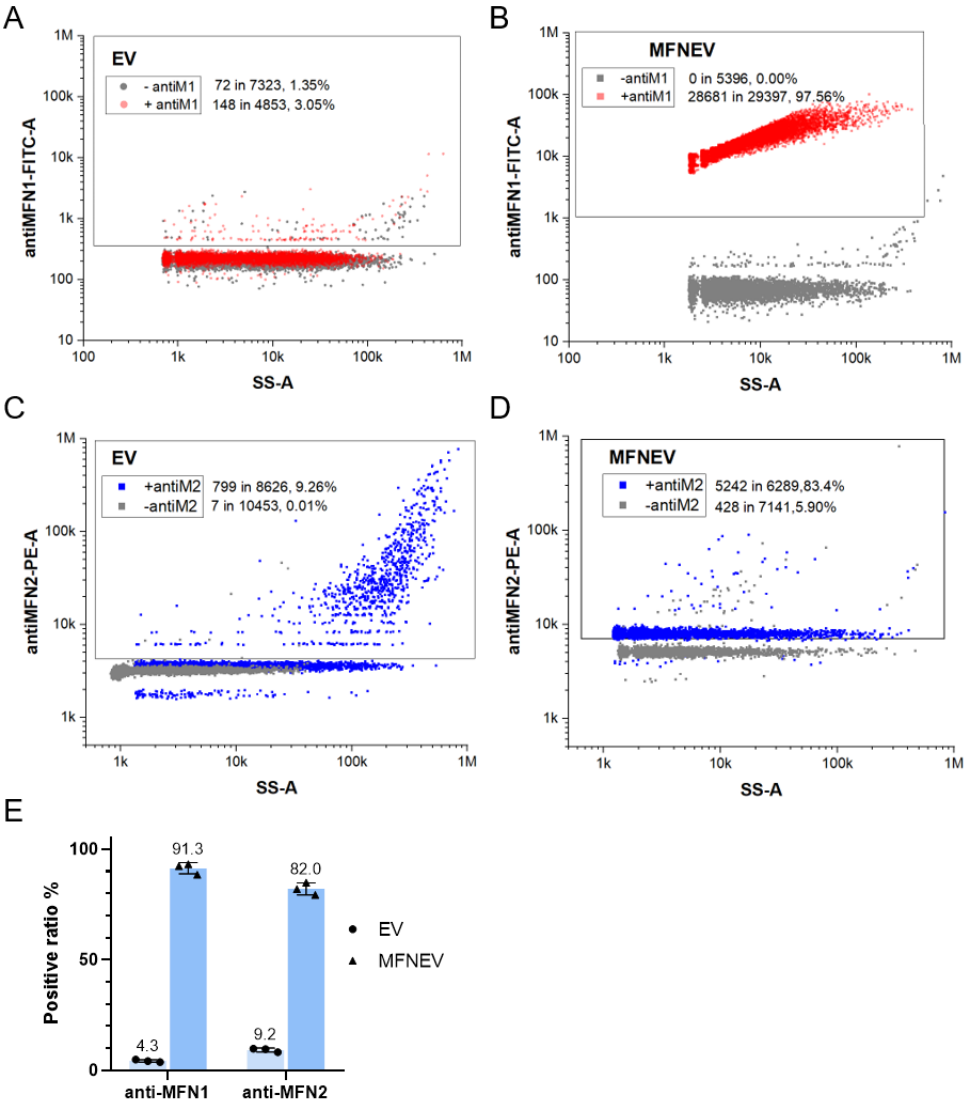

Figure S4. Analysis of the expression of MFN1-LAMP2B and MFN2-LAMP2B on EV and MFNEV. EVs or MFNEVs were incubated with antiMFN1-FITC and antiMFN2-PE antibodies and analyzed by Flow NanoAnalyzer. (**A**), (**B**) The positive ratio of MFN1-LAMP2B on EV and MFNEV. (**C**), (**D**) The positive ratio of MFN2-LAMP2B on EV and MFNEV. Each scatter dot represents an EV or MFNEV particle that was detected. MFN1 or MFN2 positive vesicles were calculated and outlined by the rectangle. (**E**) Quantification of MFN1- and MFN2-positive EVs and MFNEVs across independent batches.

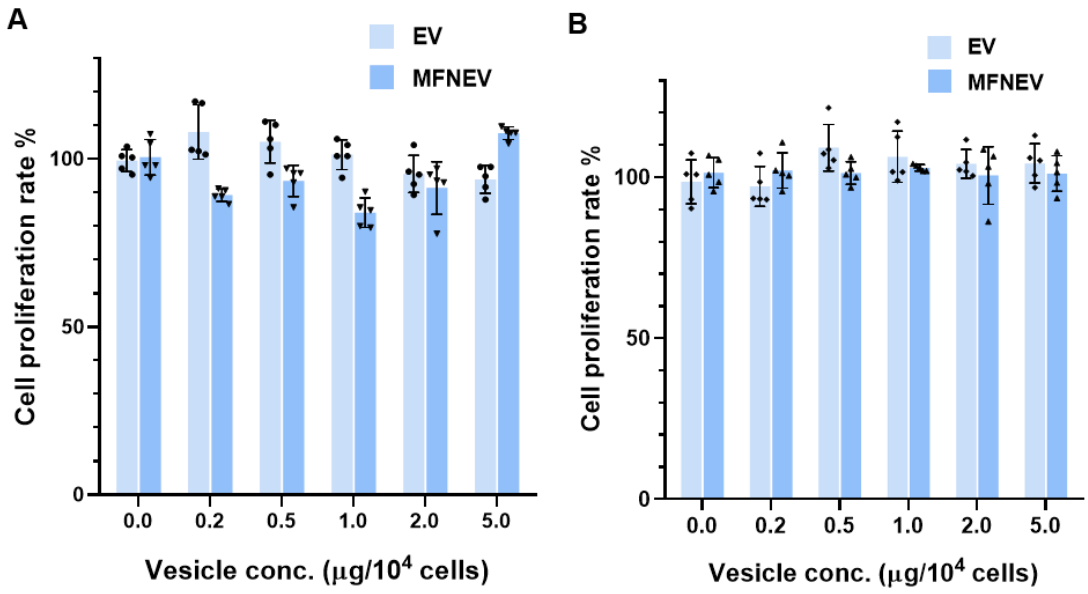

Figure S5. Effect of MFNEV on cell proliferation. HEK 293T cells were incubated with EVs or MFNEVs at indicated concentrations (covering the work concentration for the following experiments) and the cell proliferation rate was detected after (**A**) 48 h and (**B**) 72 h by Cell Counting Kit-8 (CCK8) assay.

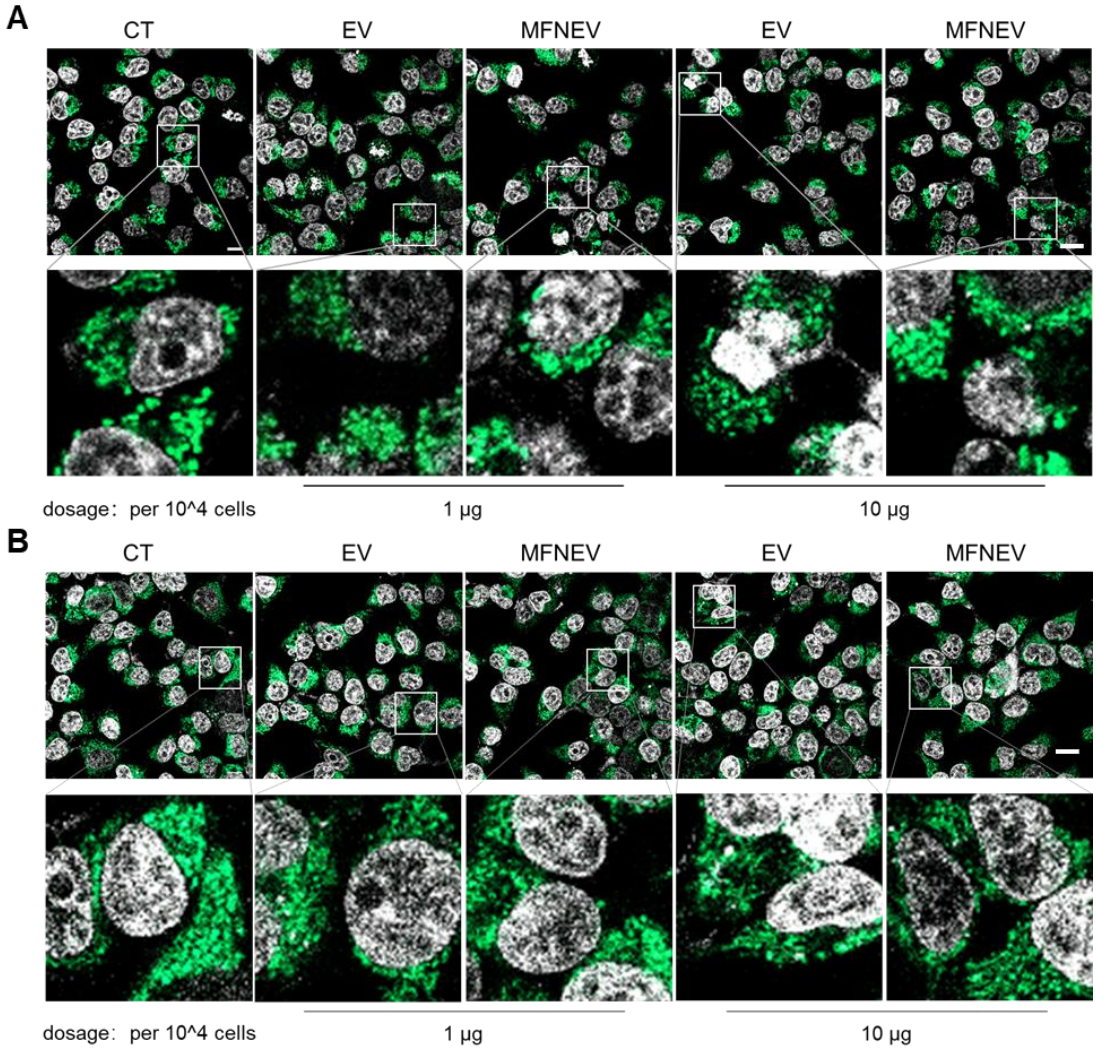

Figure S6. Evaluation of mitochondrial morphology after EV or MFNEV treatment. HEK 293T-mitoGFP cells were treated with EVs or MFNEVs at 1 μg per 10^4 cells (working dose) or 10 μg per 10^4 cells (10× dose) for (**A**) 4 h and (**B**) 12 h. Mitochondria (green) were imaged by confocal microscopy; nuclei were stained with NucBlue (gray). Scale bars, 10 μm.

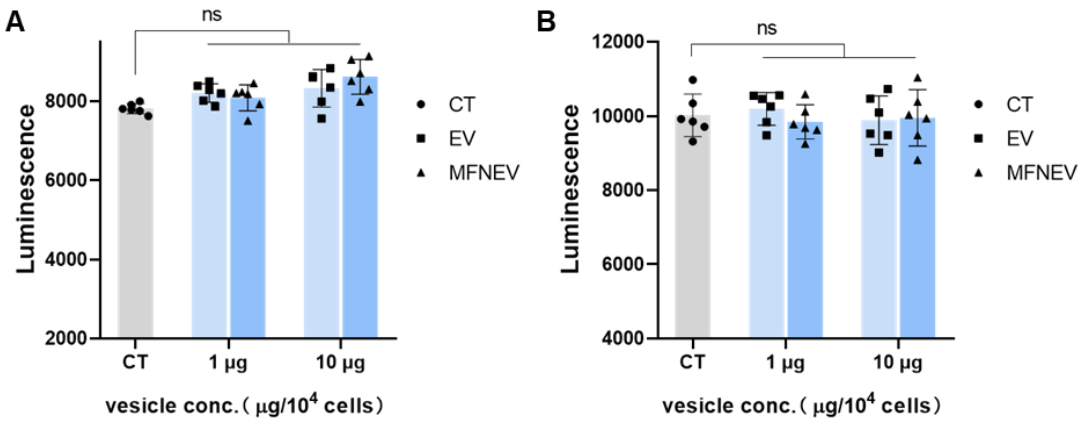

Figure S7. The effect of MFNEVs on cellular ATP levels. HEK 293T cells were treated with EVs or MFNEVs at 1 μg per 10^4 cells (working dose) or 10 μg per 10^4 cells (10× dose) for (**A**) 12 h and (**B**) 24 h. Cellular ATP was measured by a luminescence assay and normalized to cell viability. Data are presented as mean ± SD (n = 6). Statistical significance was determined by one-way ANOVA; ns, not significant.

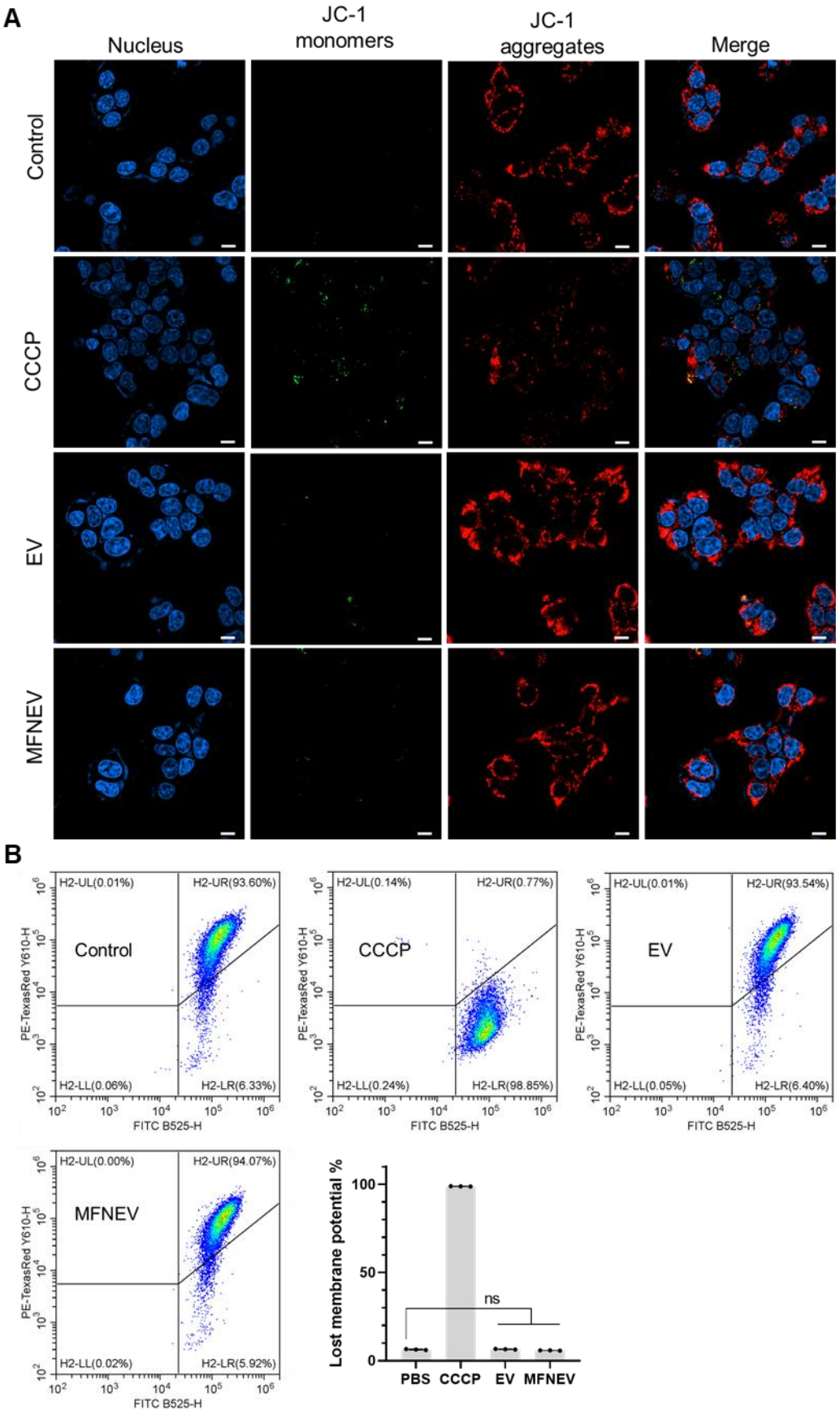

Figure S8. The effect of MFNEVs on mitochondrial membrane potential. HEK

293T cells were treated with EVs or MFNEVs at 1 μg per 10^4 cells for 24 h. Membrane potential was assessed using the JC-1 assay and evaluated by (**A**) confocal microscopy and (**B**) flow cytometry. Carbonylcyanide 3-chlorophenylhydrazone (CCCP) was used as a positive control for membrane potential dissipation. Scale bars, 10 μm. Data are presented as mean ± SD (n = 3). Statistical significance was determined by one-way ANOVA; ns, not significant.

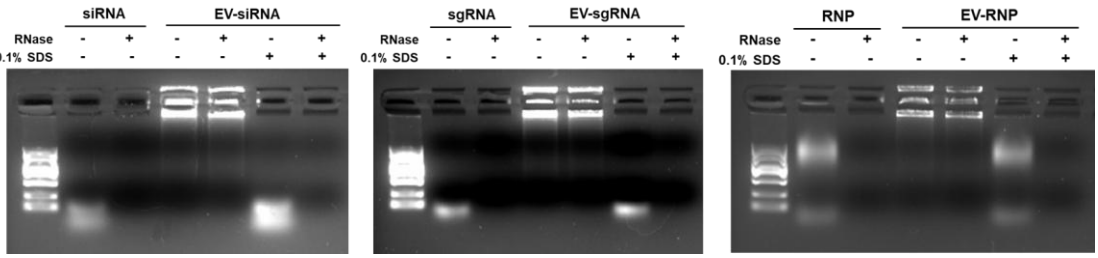

Figure S9. Validation of siRNA, sgRNA and RNP loading into MFNEVs. MFNEVs packaged with siRNA, sgRNA or RNP were purified and treated with RNase in the presence or absence of SDS, followed by agarose gel electrophoresis.

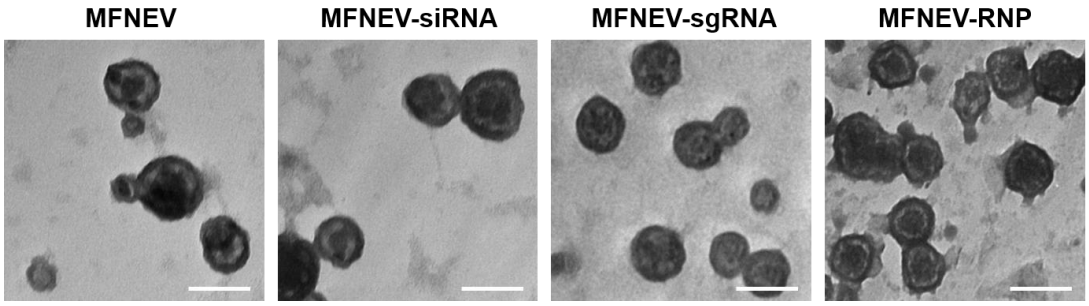

Figure S10. Morphological characterization of MFNEVs post-electroporation. Representative transmission electron microscopy (TEM) images of unloaded MFNEVs and MFNEVs after packaging with siRNA, sgRNA, or Cas9 RNP. Scale bars: 100 nm.

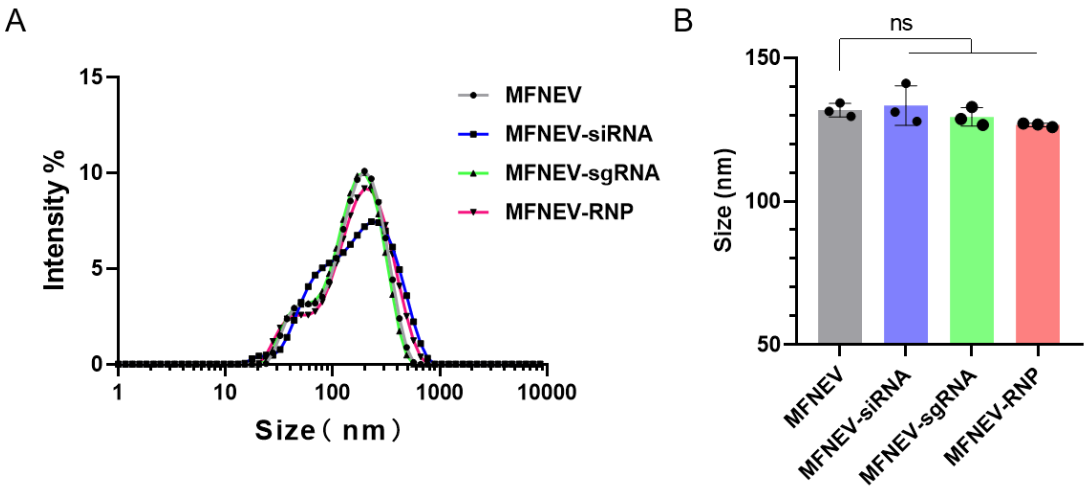

Figure S11. Size distribution of MFNEVs post-electroporation. (A) Hydrodynamic size distribution profiles and (B) quantification of the mean size of unloaded MFNEVs and MFNEVs after packaging with siRNA, sgRNA, or Cas9 RNP, as measured by dynamic light scattering (DLS). Data are presented as mean ± SD (n = 3). Statistical significance was determined by one-way ANOVA; ns, not significant.

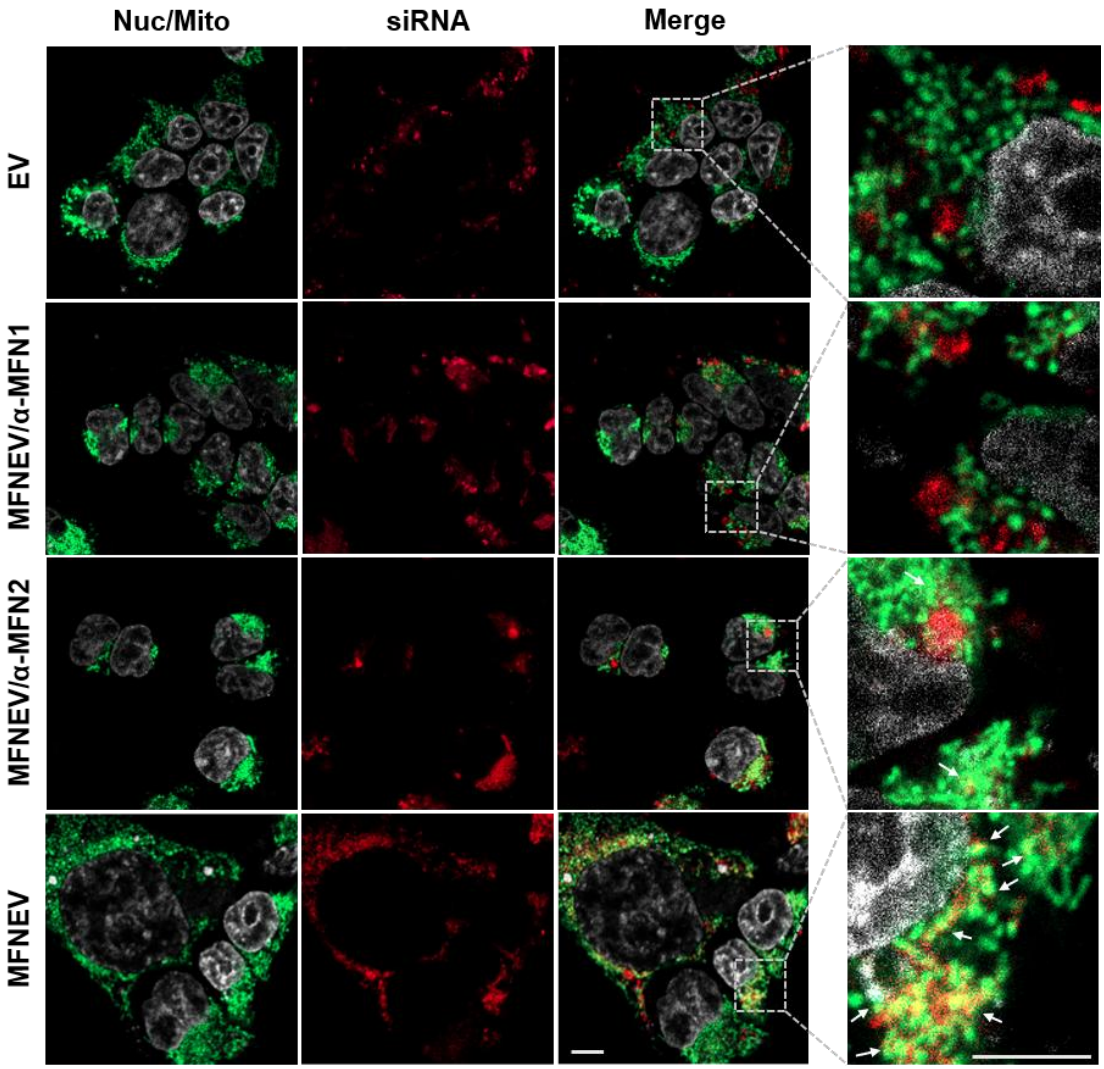

Figure S12. Colocalization of MFNEVs and mitochondria. Fluorescence microscopy images of HEK 293T-mitoEGFP cells 12 h after treating with EVs or MFNEVs. Cy5-labeled siRNA (red) was loaded into EVs and MFNEVs for intracellular tracing. MFNEVs were incubated with or without anti-MFN1 (MFNEV/α-MFN1) and anti-MFN2 (MFNEV/α-MFN2) antibodies before adding to the cell culture. The cells were stained with NucBlue (gray). Mito (mitoEGFP, green) indicates the mitochondria. The white arrows point to typical colocalizations of siRNA with mitochondria. Scale bars, 10 μm.

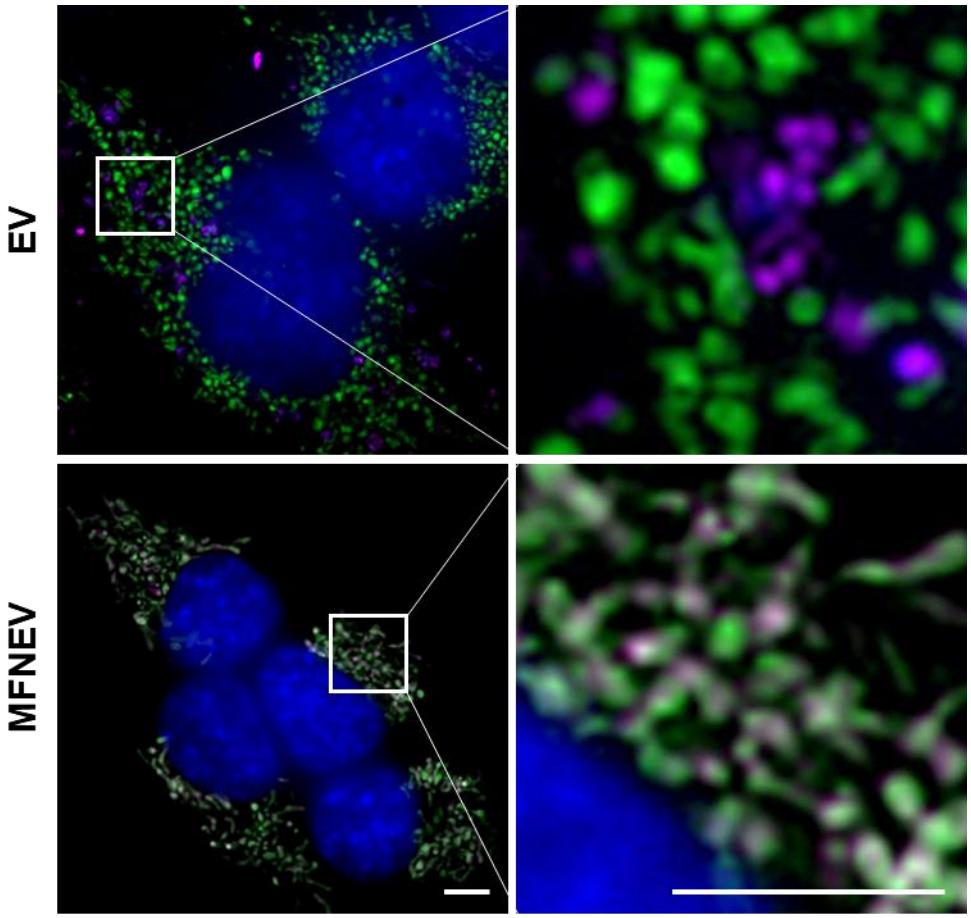

Figure S13. Colocalization of the vesicles with mitochondria by Multi-SIM. EVs or MFNEVs were loaded with Cy5-siRNA (purple). Mitochondria are labeled by mitoEGFP (green) and nuclei were stained with NucBlue (blue). Scale bars, 5 μm. Although SIM imaging can in principle resolve mitochondrial substructures, the resolution achieved in our current dataset does not allow unambiguous discrimination of submitochondrial compartments; therefore, these data are interpreted as indicating mitochondrial association or close spatial overlap.

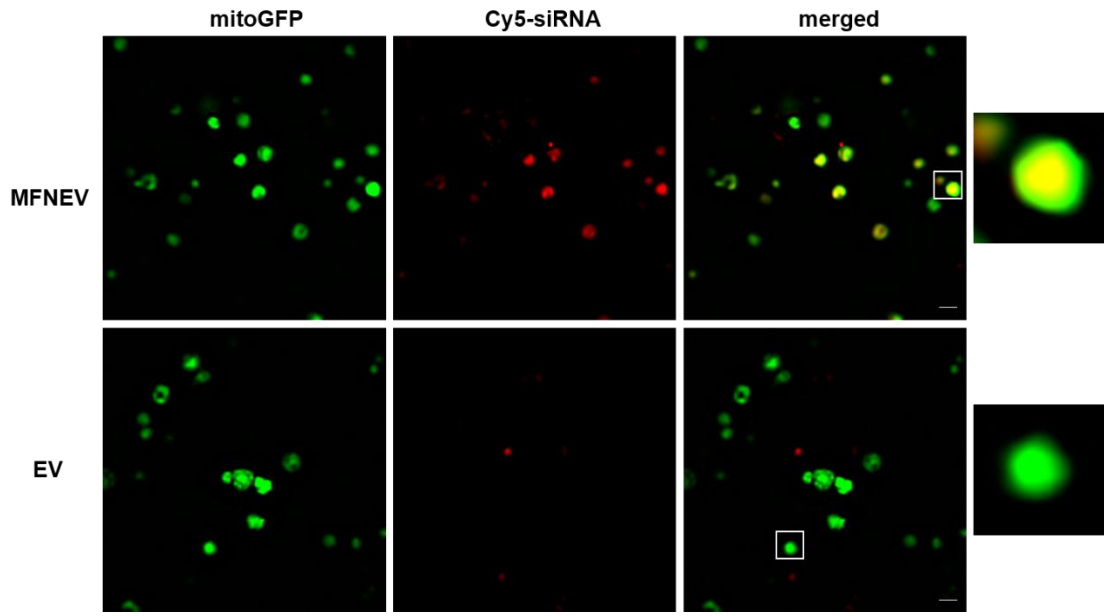

Figure S14. Mitochondria-siRNA colocalization analysis by Multi-SIM. EVs or MFNEVs were packaged with Cy5-siRNA and then incubated with 293T-mitoGFP cells. The mitochondria were isolated after 20 h for Multi-SIM imaging. In the MFNEV-treated group, Cy5-siRNA signals (red) show strong colocalization with mitochondrial regions labeled by mitoGFP (green) in isolated mitochondria, consistent with intramitochondrial localization in a reduced-background system. Scale bar: 1 μm.

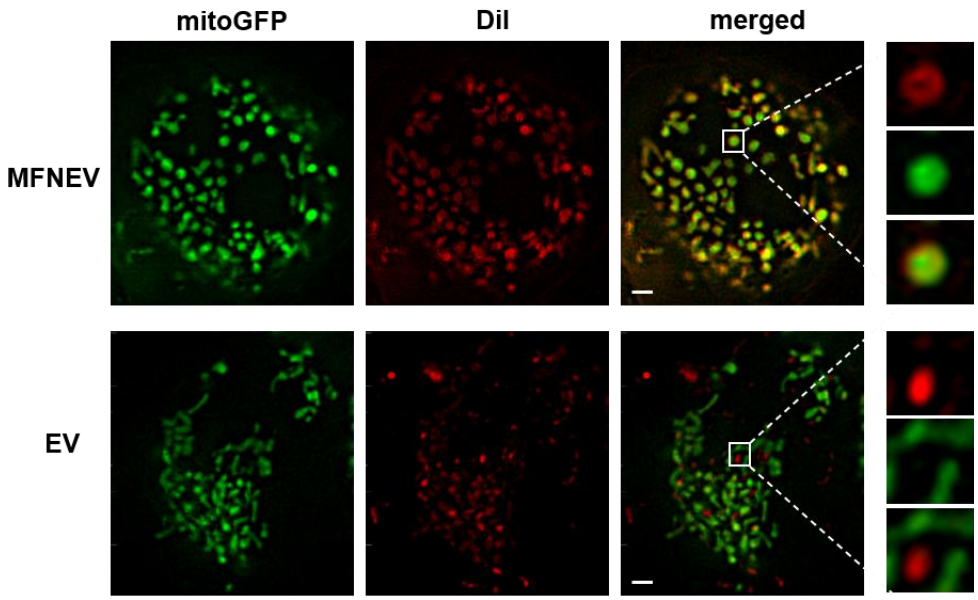

Figure S15. Mitochondria colocalization analysis by Multi-SIM. EVs or MFNEVs were labeled with DiI and incubated with 293T-mitoGFP cells for 45 min. The images show the DiI fluorescence (Red) tightly surrounded the mitochondrial matrix (mitoGFP, green) in the MFNEV treated cells, while the two fluorescence were clearly separated in the EV group. Scale bar: 1 μm.

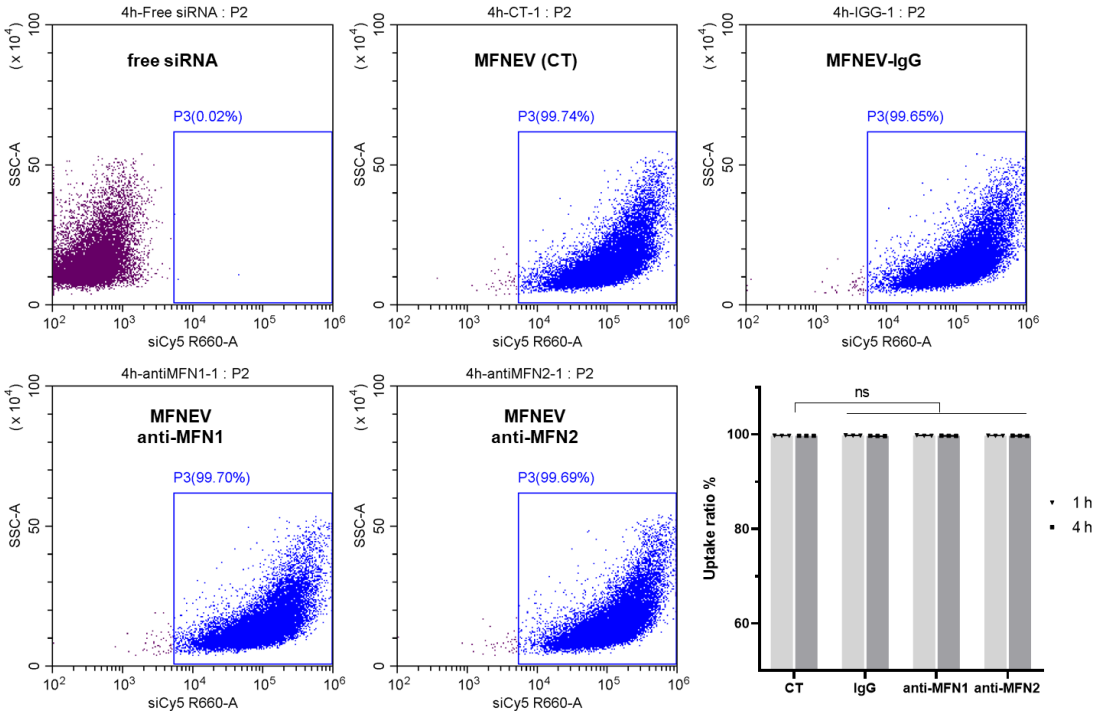

Figure S16. Cellular uptake of MFNEVs. MFNEVs packaged with Cy5-siRNA were pre-incubated with anti-MFN1, anti-MFN2 or isotype-matched control antibody (IgG). Cellular uptake was quantified by flow cytometry after 1 h and 4 h incubation. Data are presented as mean ± SD (n = 3). Statistical significance was determined by one-way ANOVA; ns, not significant

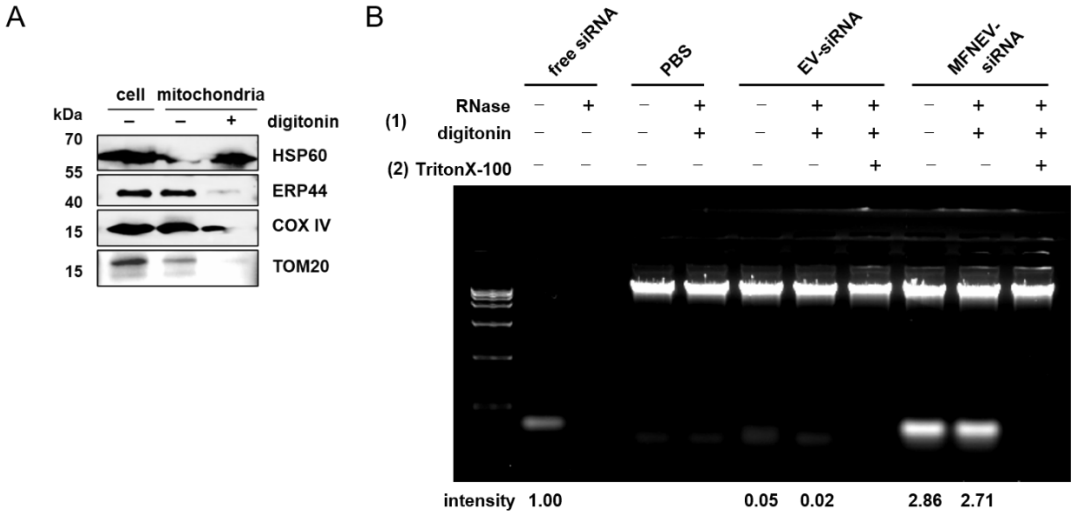

Figure S17. Detection of siRNA in mitochondria by a nuclease protection assay. Isolated mitochondria were treated with digitonin to remove the outer membrane, followed by RNase treatment to degrade unprotected siRNA. Triton X-100 was used to disrupt mitochondrial integrity. (**A**) Western blotting of isolated mitochondrial fractions for Tom20 (mitochondrial outer membrane protein), COX IV (mitochondrial inner membrane protein), HSP60 (mitochondrial matrix protein), and ERP44 (endoplasmic reticulum protein). (**B**) Agarose gel electrophoresis of siRNA associated with isolated mitochondria from the indicated groups. Free siRNA (25 ng) was loaded as a control. The relative intensity of the siRNA band was calculated by Image J.

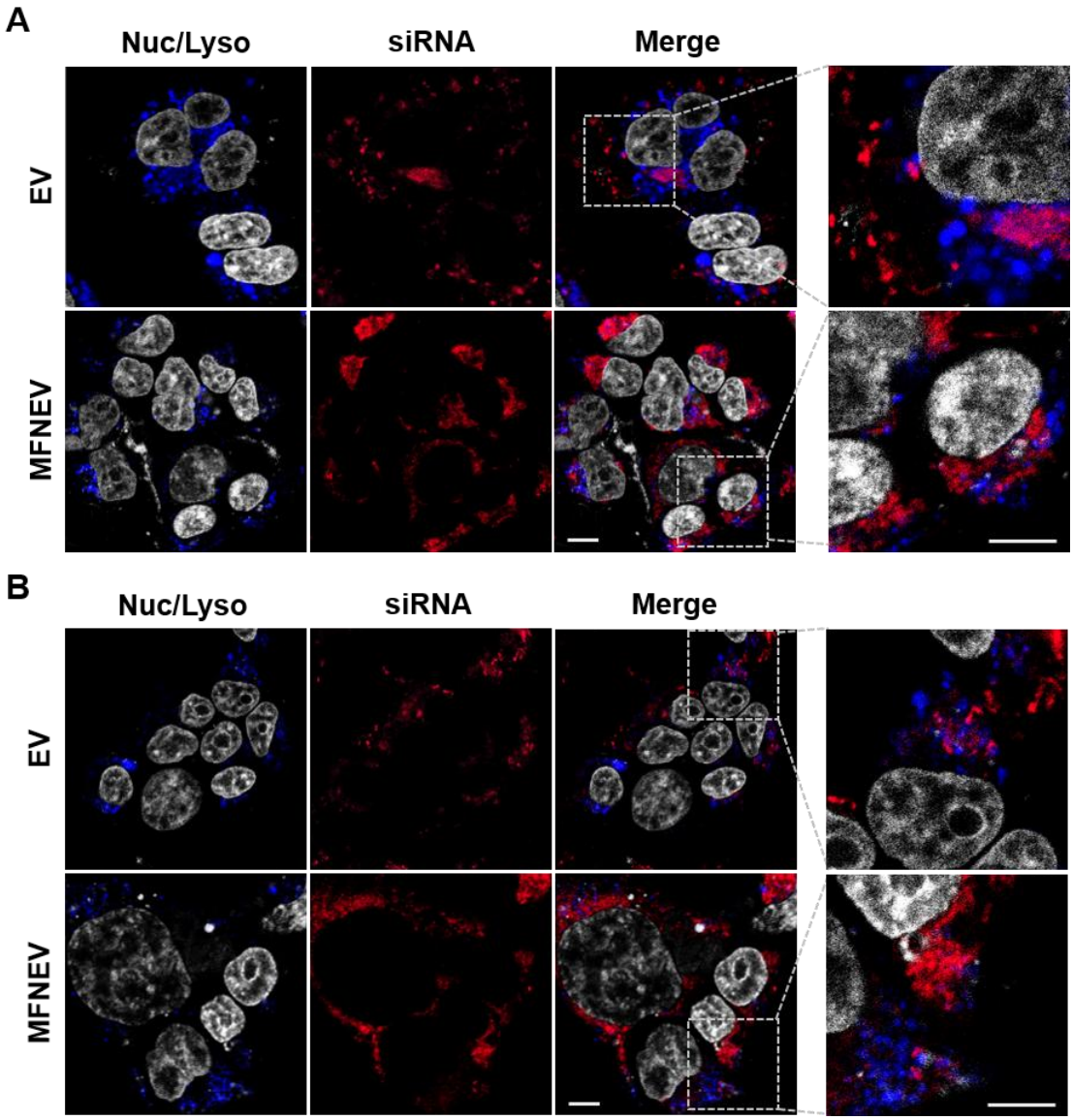

Figure S18. Colocalization of MFNEVs and lysosome. HEK 293T-mitoEGFP cells were treated with EVs or MFNEVs. Cy5-labeled siRNA (red) was loaded into EVs and MFNEVs for intracellular tracing. The cells were stained with NucBlue (gray) and LysoTracker DN99 (Lyso, blue). Fluorescence microscopy images were captured at (**A**) 4 h and (**B**) 12 h post treatment. Scale bars, 10 μm.

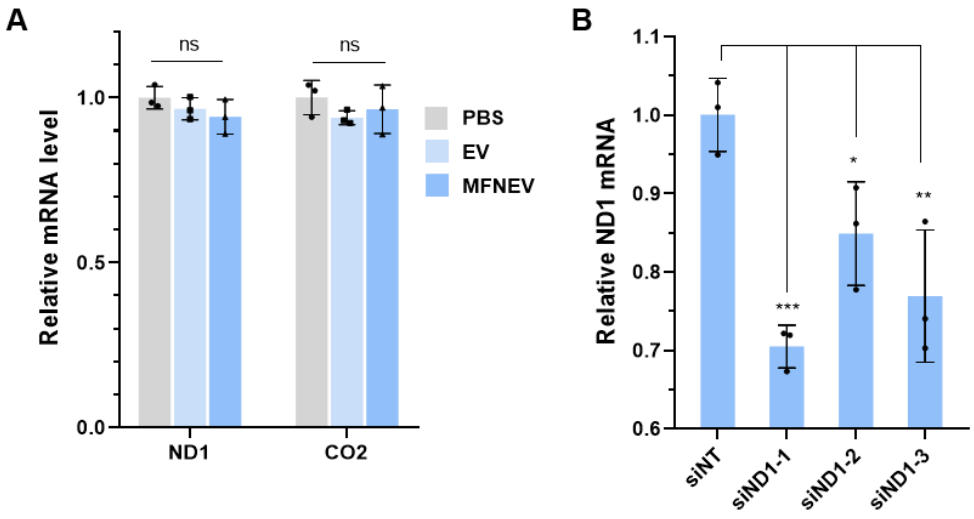

Figure S19. Quantitative PRC detection for (**A**) HEK 293T cells treated with empty EVs or MFNEVs and (**B**) HeLa cells treated with siND1 loaded MFNEVs. The relative mRNA level were presented as the mean ± SD (n = 3). Statistical significance was determined by one-way ANOVA. **P* < 0.05; ***P* < 0.01; ****P* < 0.001; ns, not significant.

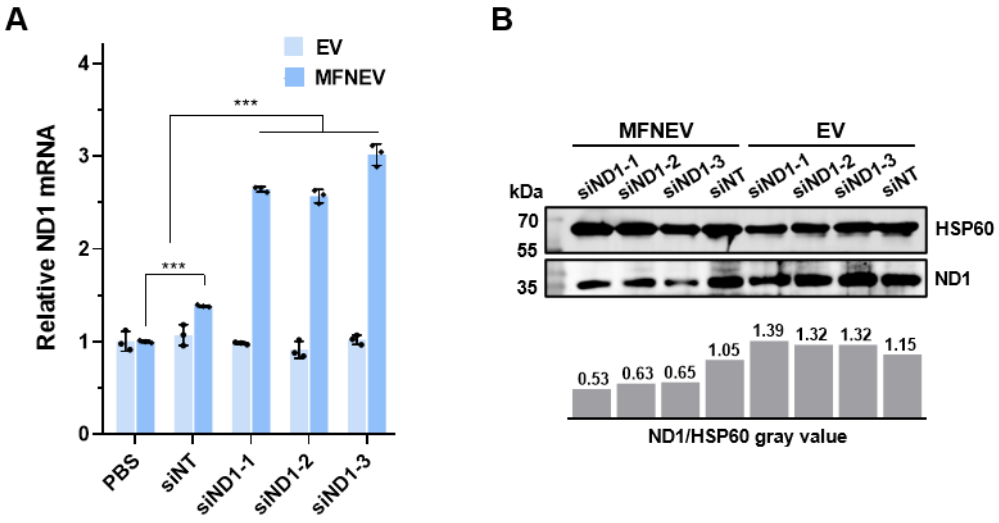

Figure S20. (**A**) Relative ND1 mRNA levels in HEK 293T cells treated with MFNEVs (30 pmol siND1 per 4×10^5 cells). Statistical significance was determined by one-way ANOVA, ***P < 0.001. (**B**) Immunoblotting of ND1 protein expression 48 hours after treatment with 5 pmol siND1-loaded MFNEVs or EVs. The mitochondrial matrix protein HSP60 was used as control.

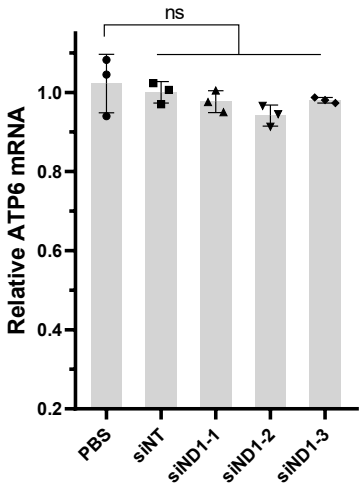

Figure S21. Quantification of the relative ATP6 mRNA. ATP6 mRNA was quantified by RT-qPCR in samples treated with MFNEVs loaded with ND1 siRNA (normalized to 16S rRNA). Data are presented as mean ± SD (n = 3). Statistical significance was determined by one-way ANOVA; ns, not significant.

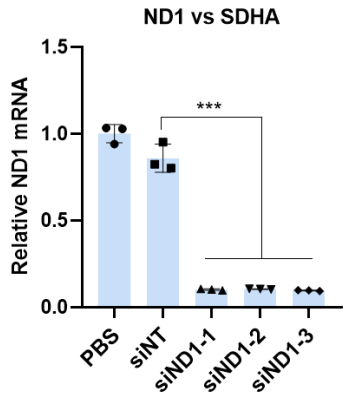

Figure S22. Efficacy of MFNEV-mediated ND1 knockdown validated by a nuclear internal control. Relative ND1 transcript levels in cells following treatment with PBS, non-targeting siRNA (siNT), or three distinct ND1-targeting siRNAs (siND1-1, siND1-2, siND1-3) delivered by MFNEVs. ND1 expression was normalized to the nucleus-encoded reference gene SDHA to accurately assess RNAi activity and rule out confounding effects from potential fluctuations in total mtDNA. Data are presented as mean ± SD (n = 3). Statistical significance was determined by one-way ANOVA. ****P* < 0.001

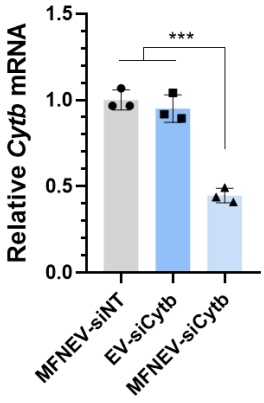

Figure S23. Quantification of the relative Cytb mRNA in isolated liver mitochondria. The mitochondria was isolated from the liver tissue of mice treated with EV-siRNA or MFNEV-siRNA. Cytb mRNA was quantified by RT-qPCR and the 16S rRNA was used as the reference. Data are presented as mean ± SD (n = 3). Statistical significance was determined by one-way ANOVA, ***P < 0.001.

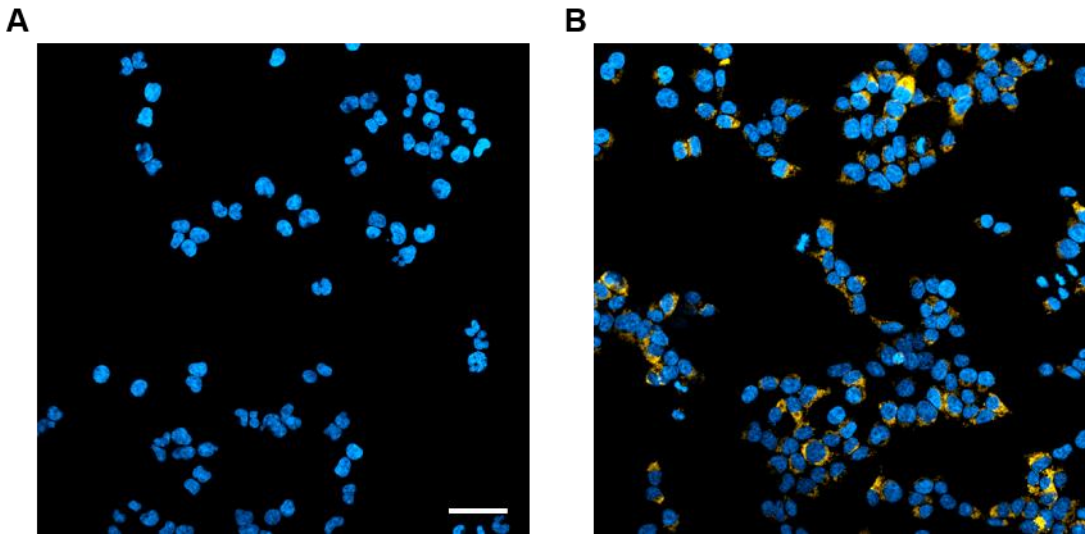

Figure S24. Immunofluorescence detection for Cas9 expression. (**A**) HEK 293T or (**B**) HEK 293T mitoCas9 cells were fixed and incubated with anti-Cas9 primary antibody and Cy3-conjugated anti-mouse IgG (yellow) sequentially, and stained with NucBlue (blue) before observing under ZEISS 980 confocal microscopy. Scale bar 50 μm.

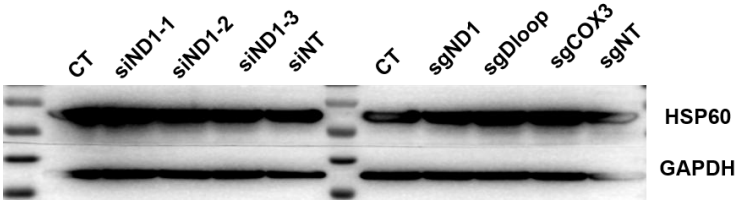

Figure S25. Stable mitochondrial matrix protein expression following MFNEV-mediated delivery. Western blot analysis evaluating the expression of HSP60 (a highly abundant mitochondrial matrix protein) in cells treated with various MFNEV-delivered siRNAs (left panel) or sgRNAs (right panel). The whole-cell protein GAPDH was used as a loading control. The consistent HSP60 levels across all treatment groups, including targeting and non-targeting (siNT/sgNT) controls, relative to the untreated control (CT), indicate the absence of generalized mitochondrial loss or global organelle degradation induced by the delivery process.

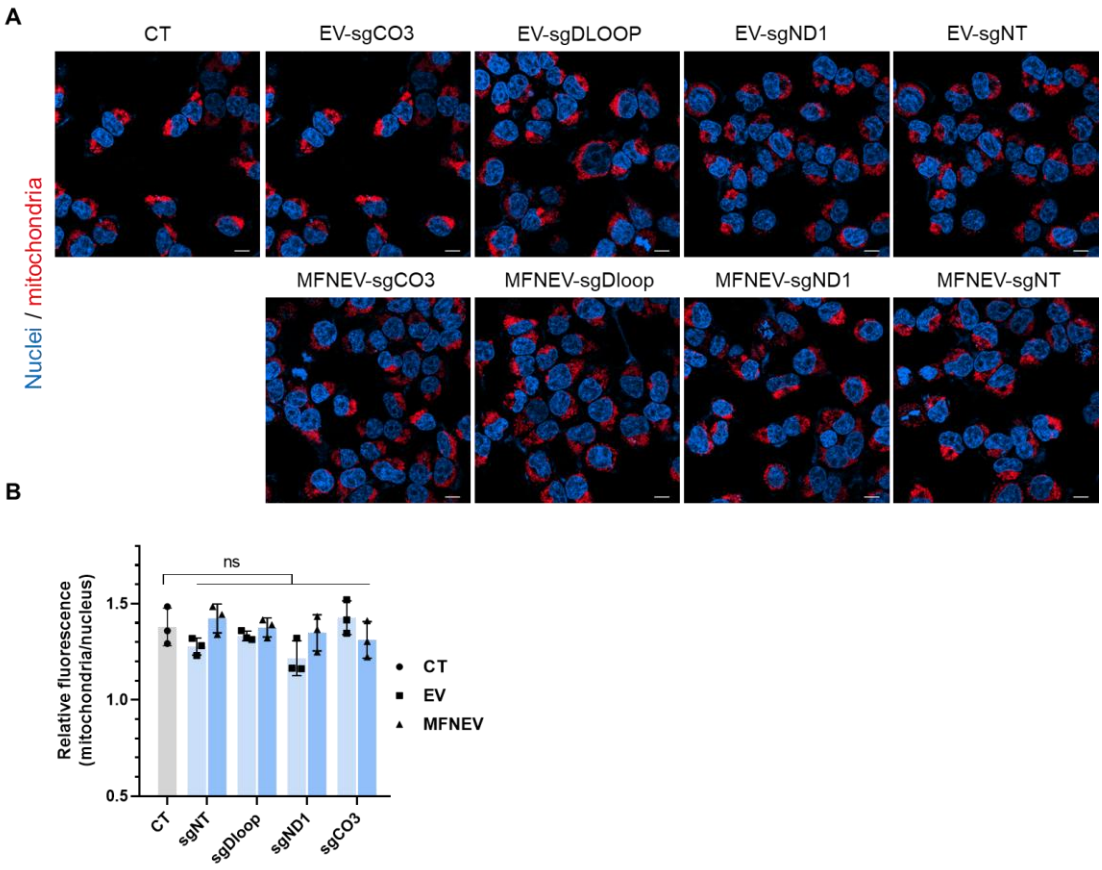

Figure S26. MitoTracker-based assessment of mitochondrial abundance in HEK293T-mitoCas9 cells. (**A**) Cells were treated with EVs or MFNEVs packaged with sgRNAs for 16 h. Mitochondria were stained with mitoTracker deepRed (red), and the nucleus was stained with NucBlue (blue). Scale bars, 10 μm. (**B**) The fluorescence intensities of mitochondria and nucleus from different views of pictures were quantified from multiple fields, and the mitochondria-to-nucleus fluorescence ratio is shown as a relative measure of mitochondrial abundance. Data are presented as mean ± SD (n = 3). Statistical significance was determined by one-way ANOVA; ns, not significant.

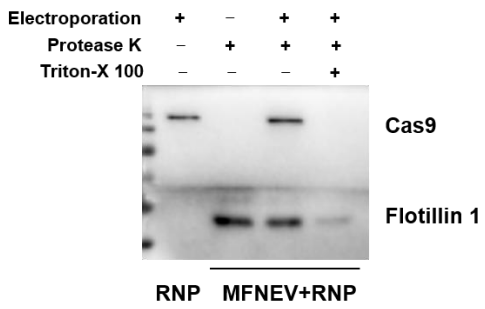

Figure S27. Validation of Cas9 RNP encapsulation via protease protection assay. Following electroporation, MFNEVs loaded with Cas9 RNPs were purified by density gradient centrifugation and subjected to Proteinase K digestion in the presence or absence of Triton X-100. Immunoblotting was performed for Cas9 and the intra-vesicular EV marker Flotillin-1.

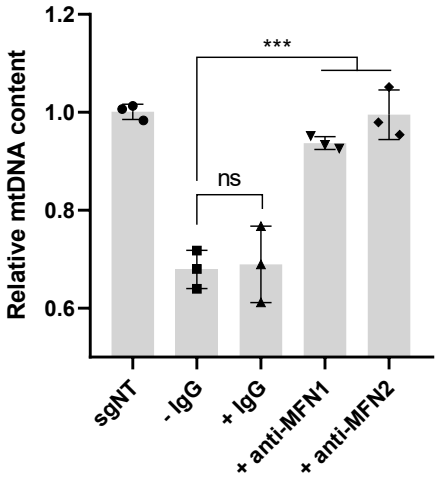

Figure S28. Specificity of MFN-mediated RNP delivery. MFNEVs packaged with the Cas9/sgND1 ribonucleoprotein (RNP) complex were pre-incubated with anti-MFN1, anti-MFN2, or isotype control (IgG) antibodies prior to addition to HEK 293T cell cultures. The relative mtDNA content was quantified by qPCR after 16 h. Data are presented as mean ± SD (n = 3). Statistical significance was determined by one-way ANOVA. ***P < 0.001; ns, not significant.

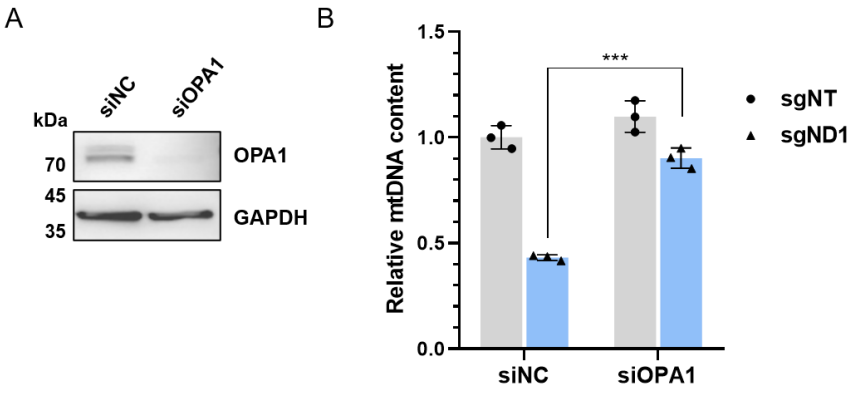

Figure S29. sgRNA delivery after OPA1 knockdown. (A) Immunoblotting validation of OPA1 knockdown at the protein level. (B) Quantification of the relative mtDNA content after sgRNA delivery in OPA1-knockdown 293T-mitoCas9 cells. Data are presented as mean ± SD (n = 3). Statistical significance was determined by one-way ANOVA; ***P < 0.001.

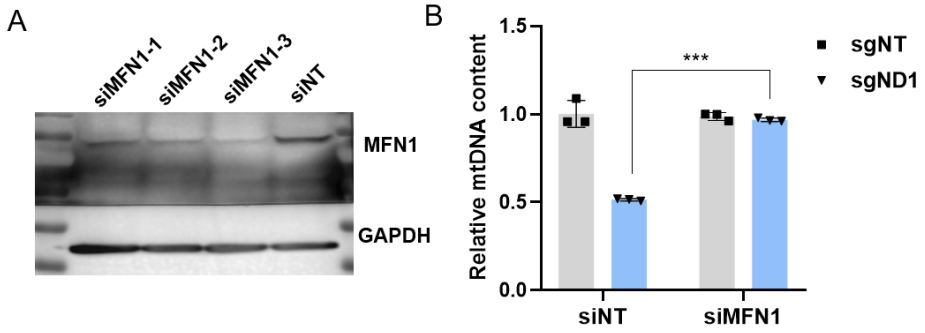

Figure S30. sgRNA delivery after MFN1 knockdown. (A) Immunoblotting validation of MFN1 knockdown at the protein level. (B) Quantification of the relative mtDNA content after sgRNA delivery in MFN1-knockdown 293T-mitoCas9 cells. Data are presented as mean ± SD (n = 3). Statistical significance was determined by one-way ANOVA; ***P < 0.001.